

# EVIDENCE OF SMALL SCALE RECONNECTION IN A MOVING FEATURE

Stéphane Régnier<sup>1</sup> and Richard C. Canfield<sup>2</sup>

<sup>1</sup>*ESA Research and Scientific Support Department, Keplerlaan 1, 2201 AZ Noordwijk, The Netherlands*

<sup>2</sup>*Physics Department, Montana State University, 264 EPS Building, Bozeman MT 59717, USA*

## ABSTRACT

Solar flares are often related to photospheric motions of magnetic polarities such as moving magnetic features (MMFs), sunspot rotation, cancelling magnetic features. Small scale changes in the magnetic field configuration due to photospheric motions should play an important role in the buildup of magnetic energy preceding flares or coronal mass ejections (CMEs) as well as to maintain the heating of the corona. We investigate these coronal changes by studying the time evolution of an active region. In active region 8210 observed on May 1st 1998, a newly emerged polarity was associated with a fast photospheric displacement. To understand the coronal response to this photospheric motion, we study the time evolution of the coronal magnetic field configuration in the vicinity of the MMF. We assume that the evolution of the magnetic field can be described by a series of nonlinear force-free equilibria. The MMF has emerged in a pre-existing magnetic configuration containing a null point and a separatrix surface. The photospheric motion has moved the MMF towards the separatrix surface. As evidenced by the evolution of the reconstructed magnetic field, the above motion has led to small scale reconnection process near the separatrix surface.

Key words: Sun: magnetic field; Sun: magnetic reconnection; Sun: flare.

## 1. INTRODUCTION

To understand the storage and the release of magnetic energy in the solar corona and especially in active regions, we need to find what are the precursors of eruptive events and how the magnetic energy can be stored and/or released even at small scale (compared to the active region size). To deal with these problems, we suggest a new method to follow the time evolution of an active region by successive nonlinear force-free equilibria based on a time series of observed photospheric vector magnetograms. The nonlinear force-free assumption allows to

have a better determination of the coronal magnetic configuration and of the free magnetic energy budget (difference between the magnetic energy of the nonlinear force-free field and of the potential field) by including a realistic contribution of the twist and of the shear from photospheric vector magnetograms.

In the following, we focus on the fast motion of an emerging parasitic polarity in a pre-existing magnetic configuration. The existence of such polarity is often considered as a precursor of eruptive events.

## 2. DATA AND METHOD

### 2.1. Time series of IVM vector magnetograms

We focus our study on the highly flare-productive active region 8210 observed on May 1st 1998 between 17:00 UT and 21:30 UT near the disc center. For this time period, a time series of vector magnetograms recorded by MSO/IVM (Mickey et al., 1996) is available. The reduction process as well as the main characteristic of this dataset are described in detail in Régnier & Canfield (2005). In order to follow the time evolution of the active region, we cross-correlate the images. Each photospheric vector magnetogram corresponds to the same surface which means that the same coronal volume is used to compute the nonlinear force-free field.

### 2.2. Vector potential Grad-Rubin-like reconstruction method for nonlinear force-free fields

To determine the magnetic configurations, we assume that the magnetic field is force-free in the corona (low plasma  $\beta$ ). The definition of the force-free field is given by the two following equations:

$$\vec{\nabla} \wedge \vec{B} = \alpha \vec{B}, \quad (1)$$

$$\vec{B} \cdot \vec{\nabla} \alpha = 0. \quad (2)$$

For a nonlinear force-free field,  $\alpha$  is a function of the position and is a constant along a given field line as shown by Eqn. (2). To solve the boundary value problem associated with these equations, we use the numerical scheme proposed by Grad & Rubin (1958). The method was rewritten by Amari et al. (1997, 1999) in terms of the vector potential  $\vec{A}$  ( $\vec{B} = \vec{\nabla} \wedge \vec{A}$ ) to insure the solenoidal condition ( $\vec{\nabla} \cdot \vec{B} = 0$ ). The Grad & Rubin iterative scheme can be written as follows:

$$\vec{\nabla} \wedge \vec{A}^{(n)} \cdot \vec{\nabla} \alpha^{(n)} = 0 \quad \text{in } \Omega, \quad (3)$$

$$\alpha^{(n)}|_{\partial\Omega^\pm} = \alpha_0 \quad \text{on } \partial\Omega \quad (4)$$

where  $\Omega$  is the coronal volume and  $\partial\Omega$  is the associated boundary and

$$-\Delta \vec{A}^{(n+1)} = \alpha^{(n)} \vec{\nabla} \wedge \vec{A}^{(n)} \quad \text{in } \Omega, \quad (5)$$

$$\vec{A}_t^{(n+1)} = \vec{\nabla}^\perp \chi \quad \text{on } \partial\Omega, \quad (6)$$

$$\partial_n \vec{A}_n^{(n+1)} = 0 \quad \text{on } \partial\Omega, \quad (7)$$

$$\lim_{|r| \rightarrow \infty} |\vec{A}^{(n+1)}| = 0. \quad (8)$$

In the above systems of equation,  $\alpha_0$  is the distribution of  $\alpha$  derived from the data and monotonically increased during the iterative process. This method corresponds to a slow injection of electric current density inside the magnetic configurations. The result of this method is to improve the stability and the convergence of the code. The operator  $\vec{\nabla}^\perp$  is defined on  $\partial\Omega$  such as  $\vec{\nabla}^\perp \cdot \vec{\nabla} = 0$ .  $\chi$  is the unique solution of

$$-\Delta_\perp \chi = b_0 \quad \text{on } \partial\Omega, \quad (9)$$

$$\chi = 0 \quad \text{or} \quad \partial_n \chi = 0 \quad \text{on } \Gamma \quad (10)$$

where  $\Delta_\perp$  is the Laplacian operator on  $\partial\Omega$  and  $\Gamma$  is the border of  $\partial\Omega$ .  $b_0$  is the magnetic field distribution of the normal component to  $\partial\Omega$ .

Practically, we use the photospheric vector magnetograms described in the previous Section to prescribe the bottom boundary conditions: the vertical component of the magnetic field in both polarities and the distribution of  $\alpha$  in one polarity. On the other sides of the computational box, we impose that  $\vec{B} \cdot \vec{n} = 0$  (same as Eqn. 8).

### 3. RECONNECTION PROCESS CAUSED BY A MOVING MAGNETIC FEATURE

In AR8210, we have observed the emergence of a negative parasitic polarity in the North-West part. In Fig. 1, this polarity is represented by the blue contours and the green field lines connecting the negative polarity and two positive polarities. The velocity of the displacement indicated by the red arrow is estimated to  $0.7 \text{ km.s}^{-1}$  towards the South-West part of the image. The scenario of the evolution is as follows. The negative polarity emerges

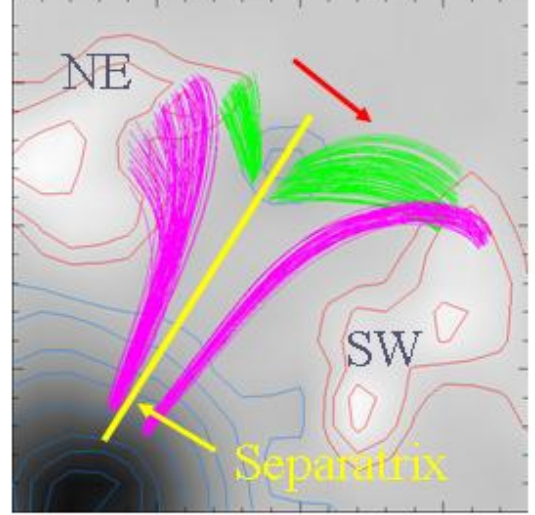


Figure 1. Topology of the magnetic field surrounding the moving magnetic feature. Red (green) field lines describe the pre-existing (emerging polarity) magnetic field. The yellow line roughly indicates the location of the separatrix surface dividing the field-of-view into two domains of connectivity (NE and SW). The red arrow indicates the displacement of the negative polarity. Red (blue) contours are the positive (negative) polarities.

in a pre-existing magnetic configuration (red field lines) having a topology (null points, separatrix surfaces). The parasitic polarity is located East of the separatrix surface and is moving towards the South-West. Therefore some field lines of the negative polarity are closer and closer to the separatrix surface. Then field lines in domain NE are reconnected in domain SW as described in Fig. 2. During the time evolution of  $\sim 4$  hours, most of the field lines connected in domain NE are reconnected into domain SW as evidenced by the time series of nonlinear force-free field configurations depicted in Fig. 2.

### 4. DISCUSSION AND CONCLUSION

We have developed a new technique to follow the time evolution of 3D magnetic field configurations of active region: we consider that the evolution can be described by a time series of nonlinear force-free equilibria based on photospheric vector magnetograms.

Using this technique, we have evidenced the occurrence of small scale magnetic reconnection. These reconnection processes do not lead to any observed coronal enhancements in  $H\alpha$  and EUV images and therefore these events cannot be responsible for the flaring activity occurring in AR8210. We have shown that the existence of a parasitic polarity and that transverse photospheric motions are precursors of reconnection processes. Nevertheless the speed of the transverse motion is too fast and the

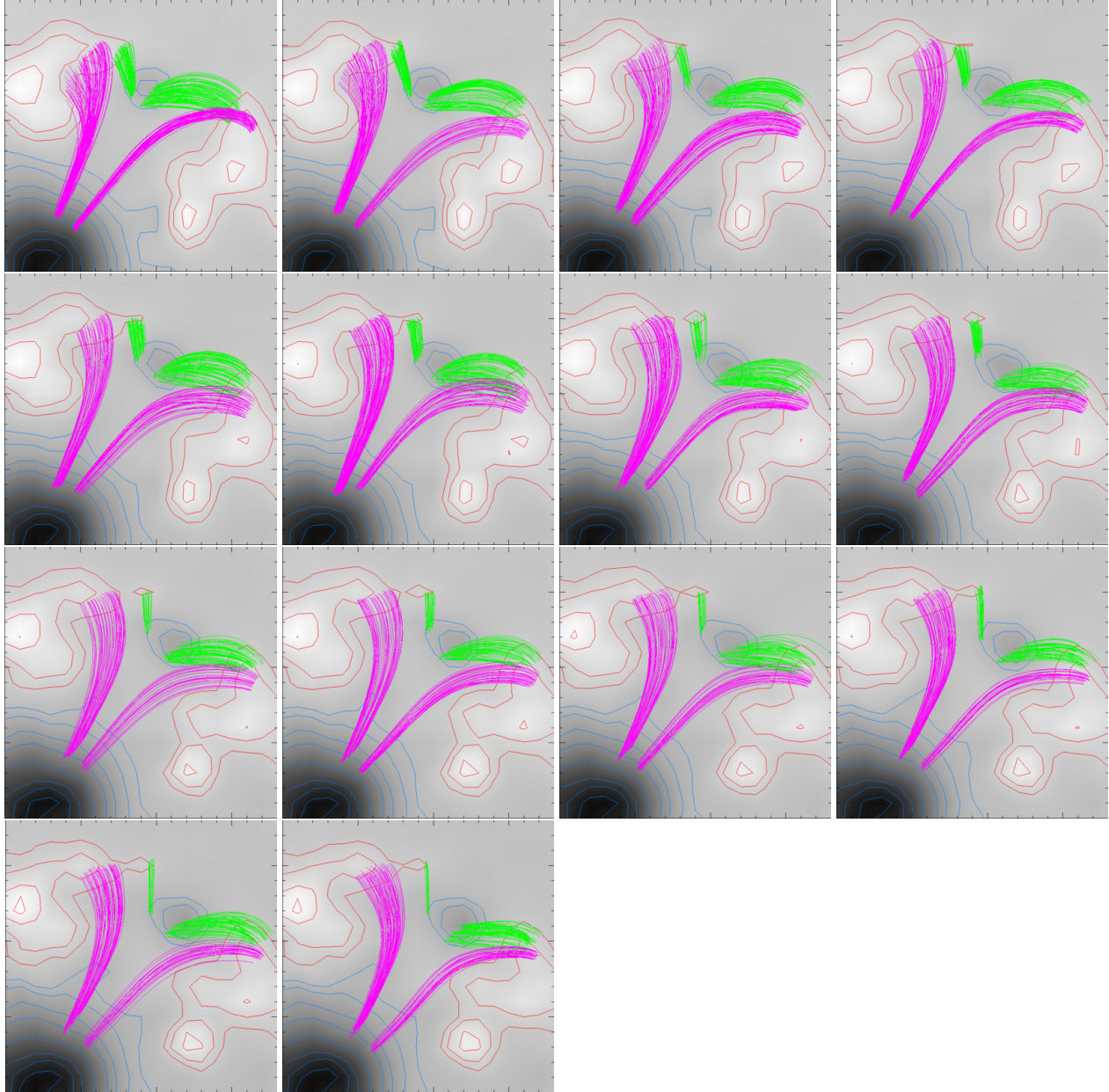


*Figure 2. Time evolution of the fast moving parasitic polarity (from left to right and row by row). Red field lines describe the pre-existing magnetic configuration in which the negative polarity has emerged (green field lines). The photospheric negative (positive) magnetic vertical field corresponds to blue (red) contours.*

scale height too small to store enough magnetic energy to trigger C-class flares.

## **ACKNOWLEDGMENTS**

S. R.'s research is funded by the European Commission's Human Potential Programme through the European Solar Magnetism Network (contract HPRN-CT-2002-00313). The computations have been performed on a V880 Sun computer supported by the DoD/AFOSR MURI grant "Understanding Magnetic Eruptions and their Interplanetary Consequences".

## **REFERENCES**

- Amari, T., Aly, J. J., Luciani, J. F., Boulmezaoud, T. Z., Mikic, Z. 1997, *Solar Phys.*, 174, 129
- Amari, T., Boulmezaoud, T. Z., Mikic, Z. 1999, *A&A*, 350, 1051
- Grad, H., Rubin, H. 1958, in *Proc. 2nd Int. Conf. on Peaceful Uses of Atomic Energy*, 31, 190
- Mickey, D. L., Canfield, R. C., Labonte, B. J., Leka, K. D., Waterson, M. F., Weber, H. M. 1996, *Solar Phys.*, 168, 229
- Régnier, S., Canfield, R. C. 2005, *A&A*, submitted